

# Exploring Valleys of Aging Systems: The Spin Glass Case

Jesper Dall and Paolo Sibani  
 Fysisk Institut, Syddansk Universitet 5230 Odense M  
 Denmark

December 26, 2019

## Abstract

We present a statistical method for complex energy landscape exploration which provides information on the metastable states—or valleys—actually explored by an unperturbed aging process following a quench. Energy fluctuations of *record* size are identified as the events which move the system from one valley to the next. This allows for a semi-analytical description in terms of log-Poisson statistics, whose main features are briefly explained. The bulk of the paper is devoted to thorough investigations of 3D Ising spin glasses with short range interactions, a well established paradigm for glassy dynamics. Simple scaling expressions for (a) barrier energies, (b) energy minima and (c) the Hamming distance as a function of the valley index are found. Finally, we investigate the distribution of residence time inside valleys entered at age  $t_w$ , and the distribution of the time at which the global minimum inside a valley is hit.

The results fit well into the framework of available knowledge about spin glass aging. At the same time they support a novel interpretation of thermal relaxation in complex landscapes with multiple metastable states. The *marginal stability* of the attractors selected is emphasized and explained in terms of geometrical properties of the landscape.

## 1 Introduction

Physical properties of glassy systems quenched from a high temperature slowly change with the time or age  $t_w$  elapsed since the quench. For any  $t_w$  well below

the true equilibration time, the dynamics deceptively appears to be stationary when observed on time scales shorter than  $t_w$ . Experimental and numerical evidence for the presence of a quasi-stationary fluctuations regime for  $t \ll t_w$  followed by non-equilibrium drift for  $t \gg t_w$ , stems e.g. from measurements of conjugate linear response and autocorrelation functions [1, 2, 3] which obey, respectively violate, the fluctuation dissipation theorem in the two regimes. In general, the (apparent) age of the system can be deduced from the decrease in the rate of change of macroscopic averages. This apparent age can however be ‘reset’ to an earlier value by applying a perturbation of short duration, as e.g. a temperature pulse, which thus rejuvenates the system.

Non-equilibrium memory effects such as aging and rejuvenation were first noticed [4, 5] and studied [6, 7] in a spin glass context, but are now observed in a variety of glassy systems [8, 9, 10, 11, 12]. Expanding a previous brief exposition [13], we describe and test a statistical approach to landscape explorations designed to find the generic properties of the energy landscape which produce these effects.

Our main point is that the dynamical events marking the transition between the quasi-equilibrium and the off-equilibrium dynamical regimes are triggered by the attainment of energy values of record magnitude. This immediately allows a description of the non-equilibrium dynamics in terms of a log-Poisson process [14], i.e. a stochastic process which is homogeneous when viewed on a logarithmic time scale.

The sequel is organized as follows: the next section introduces the landscape exploration method. Sec-

tion 3 briefly explains the relevant properties of the log-Poisson statistics used throughout the paper as a semi-analytical description of non-equilibrium dynamics. Section 4 presents results of an extensive application of the method to spin glass systems, demonstrating the viability of the method and the usefulness of the log-Poisson description. Section 5 puts the results in a broader perspective, with special reference to coarse-grained mesoscopic models of configuration space. In particular, we discuss the connection between aging in thermalizing systems and in dissipative driven system and biological evolution. Section 6 is a summary and an outlook.

As the nature of true equilibrium and the final stages of thermal relaxation are weakly related to the presented data, no theoretical consideration is given to these aspects in the paper.

## 2 The Method

In models of driven dissipative systems with multiple attractors [10, 14, 15], marginally metastable attractors with an *a priori* negligible statistical weight are nevertheless those typically selected by the dynamics. In these systems, this mechanism underlies memory and rejuvenation effects analogous to those observed in the thermalization of e.g. spin glasses [16] after a quench. One can speculate that similar mechanisms could generally be present in glassy systems with an extensive number of metastable attractors. However, the issue of attractor selection is not explicitly considered in widely used landscape exploration methods such as the Stillinger-Weber approach [17, 18, 19, 20, 21], which study a set of local energy minima (inherent states) generated by quenches. The same applies to exhaustive landscape exploration techniques [22, 23, 24] and studies of the real space morphology of low-energy excitations by techniques requiring quenches [25], genetic algorithms [26] and energy minimization of excitations of fixed volume [27, 28].

The ability of small external perturbations to induce strong rejuvenation and memory effects in complex dynamics strongly suggests that any probe introducing extraneous elements in the dynamical evo-

lution might also yield a biased picture of the energy landscape. In other words: are the attractors identified also those which would be selected by e.g. the unperturbed thermalization process after a deep quench or any other dynamical evolution of interest? Analyzing regions of state space surrounding intrinsic states provides valuable information about the quasi-equilibrium (fluctuation) dynamics in the energy landscape, but does not tell the whole story. The question of how to properly describe the non-equilibrium process of ‘selecting’ the metastable states is still open. This question motivates the present approach which is solely based on statistical information collected during an *undisturbed aging process*.

Conventionally, a valley is a connected neighborhood of configuration space which supports a state of approximate thermal equilibrium around a local energy minimum. During the time a trajectory ‘resides’ in a valley, the energy and other physical quantities fluctuate around a fixed average, and the state of lowest energy is often revisited; the dynamics has a recurrent character. Non-equilibrium events, henceforth ‘quakes’, move the system irreversibly from the neighborhood of the initial local energy minima of high value and into progressively deeper valleys. A sequence of such events seldom or never revisits the same configurations and has a transient character.

As widely recognized, the lack of time translational invariance in aging systems stems from the dynamical in-equivalence of the valleys visited. Consider therefore a landscape with multiple valleys of varying degrees of metastability, or depth. On time scales larger than the residence time of the deepest (i.e. most stable) valley seen up to the age  $t$ , all valleys shallower than this valley are, by definition, unstable and hence irrelevant for the non-equilibrium dynamics. The interesting dynamical objects are thus the valleys deeper than the deepest valley seen up to time  $t$ . This points to energy records as prospective markers of the non-equilibrium events.

We shall use the term ‘energy barrier’ to denote the difference between the energy of the current state and the lowest seen or best-so-far (bsf) energy minimum. The bsf energy minimum value and the highest or bsf energy barrier observed up to time  $t$  will identify the

valleys as they successively appear in the landscape.

Our classification procedure of the undisturbed dynamics is as follows: We save the bsf minimum and barrier values encountered and the times at which they occur. We stipulate that a valley is entered at time  $t$  if the barrier record achieved at time  $t$  happens to be the last one prior to the attainment of a bsf minimum. To leave a valley, a barrier record must again be followed by a record in the lowest energy. Whenever several minima records are found between two barrier records, we only keep the latest, and therefore deepest, minimum.

In short, we operationally identify the valleys encountered by a series of bsf minima with at least one barrier event between them. Note that this selection procedure must be performed retrospectively, since it is impossible to know ‘on the fly’ whether a new valley has been entered or not. We also stress that the barrier records will not necessarily coincide with the lowest barrier separating two consecutive bsf minima, as the dynamics, due to entropic effects, is not likely to follow the path of lowest energy, an effect noticed by Wevers et al. [29] in the landscape of metastable ionic compounds.

The discovery of a new bsf minimum is a non-equilibrium event. However, by no means does it imply that the internal dynamics in a valley is entirely equilibrium-like. Several sub-valleys are typically explored before the energy minimum is encountered which eventually remains as the lowest state within the valley. Only then does the dynamics acquire the recurrent, fluctuation-like nature which is characteristic of quasi-equilibrium.

Resetting the bsf barrier to zero at an arbitrary point in time produces numerous barrier records but no new valleys before a lower bsf energy value is again recorded. However, resetting both the bsf energy and barrier values to zero may result in a series of new records being registered, which describe sub-valleys within the valley originally explored. By repeating the simulation with the exact same random numbers, this procedure allows one to take a closer look at the internal structure of a valley if the resetting is done at the time of entry.

The method presented is generally applicable, easily implemented, and does not add much to the to-

tal runtime of a simulation. If the energy landscape explored is simple, e.g. if it contains one large, structureless valley or if it is perfectly periodic, our scheme only detects a single valley, since degenerate and hence dynamically equivalent minima are appropriately lumped together. In other words, our method produces simple results when used on simple systems. In the following sections we show that non-trivial results are indeed the outcome when complex landscapes are explored.

### 3 Log-Poisson statistics

In this section we introduce and motivate the log-Poisson statistics used through the paper as an idealized analytical description of non-equilibrium events—such as the quakes which lead to new valleys. We mainly focus on the consequences and predictions for various quantities of physical interest, leaving the empirical justification of the formalism to the next section, where the data are presented.

A log-Poisson description of complex dynamics was first introduced in connection with a model of Charge Density Waves [14], and later used to explain macroevolutionary patterns from the fossil record [30, 31]. It describes [32] the coarse grained dynamics of a population evolving in a NK landscape [33], and there are indications that it might also apply to far more realistic models of evolution [34].

The familiar Poisson process with the time argument replaced by its logarithm is in short denoted log-Poisson:

$$P_k(t) = \frac{(\alpha \ln t)^k}{k!} t^{-\alpha}, \quad t \geq 1. \quad (1)$$

As shown in [14, 31], the probability that  $k$  records occur in a sequence of  $t$  random numbers is given by Eq. (1), independently of the underlying process generating the numbers. Log-Poisson statistics implies that the tempo at which the events occur falls off as  $1/t$ . Switching to  $\log t$  as the independent variable gives a constant (logarithmic) rate of events, and restores time homogeneity. There are several other interesting mathematical properties of log-Poisson processes, which are listed below together with their

physical implications for the spin-glass problem at hand.

The probability that  $k$  ‘events’ occur in the time interval  $[t, t + \tau]$ :

$$P_k(t, t + \tau) = \frac{1}{k!} \left[ \alpha \ln \left( \frac{t + \tau}{t} \right) \right]^k \left( \frac{t + \tau}{t} \right)^{-\alpha}. \quad (2)$$

Consider a function  $C_X(k)$  describing the effect of  $k$  events, for example the decorrelation of the initial configuration. The corresponding aging behavior is given by the average

$$\overline{C_X}(t, t + \tau) = \sum_{k=0}^{\infty} C_X(k) P_k(t, t + \tau). \quad (3)$$

which is a function of  $\tau/t$  only.

This *pure* or *full* aging form has very recently been shown to describe non-equilibrium relaxation in real spin glasses, if cooling rate effects through the critical temperature are accounted for [35]. We also note that the correlation stiffens as the age  $t$  grows for fixed time, in agreement with the experimental findings. The assumption that  $\tilde{C}_X(k)$  only depends on a single argument is consistent with the time homogeneity of the log-Poisson dynamics, but must of course be verified separately. Any additional dependence of  $C_X$  on the valley index of the initial configuration entails a deviation from  $\tau/t$  scaling. As a test, we checked numerically the overlap between configurations separated by  $k$  events in 3D spin glasses and found that the simple, exponential form  $\tilde{C}_X(k) = \exp(-\gamma k) + \text{const}$  describes the decay well. With this assumption, simple algebra yields

$$\overline{C_X}(t, t + \tau) = \left( \frac{t + \tau}{t} \right)^{-\alpha(1-e^{-\gamma})} \quad \tau > t, \quad (4)$$

The condition  $\tau > t$  points to the fact that the equilibrium decorrelation taking place within the ‘initial’ valley is neglected.

For later convenience we finally note that, if  $t_k$  marks the time of the  $k$ ’th event in a log-Poisson process occurring after  $t$ , the ‘log-waiting time’  $\log(t_k) - \log(t)$  is exponentially distributed, in perfect analogy to the usual Poisson process. The same exponential

distribution also describes the series of *independent* variables  $\log(t_k) - \log(t_{k-1})$ . This property of the log-waiting time distribution is very well fulfilled by our data.

## 4 Results

As glassy dynamics is largely insensitive to the specific form of the interactions, computational convenience is a prime criterion for choosing a test model. Spin glass models are comparatively easy to simulate and have been investigated experimentally and numerically for more than twenty years. Nevertheless, a comprehensive and coherent picture of their dynamics and statics is still not in place, which endows them with considerable intrinsic interest.

This section demonstrates that a simple and consistent geometrical picture of the spin glass energy landscape is obtained with our ‘non-invasive’ exploration method. Current spin-glass issues are mentioned as needed, while a more comprehensive discussion can be found in Section 5.

We consider  $N = L^3$  Ising spins placed on a cubic lattice with periodic boundary conditions. The energy of a spin configuration  $\mathbf{s} = \{s_1, \dots, s_N\}$  is given by

$$E(\mathbf{s}) = -\frac{1}{2} \sum_{i,j} J_{ij} s_i s_j, \quad (5)$$

where the couplings  $J_{ij}$  are symmetric, independent Gaussian variables of unit variance. Restricting ourselves to short range systems,  $J_{ij}$  are non-zero only if  $i$  and  $j$  are lattice neighbors.

We use single spin flip dynamics coupled with a rejectionless algorithm, the Waiting Time Method [36]. The latter generates a sequence of moves equal in probability to the sequence of *accepted* moves in the Metropolis algorithm. Thus, the results of this paper can also be obtained with the standard Metropolis algorithm, albeit at the price of considerably longer runtimes. The ‘intrinsic’ and size independent time variable  $t$  used throughout corresponds to the number of Monte Carlo (lattice) sweeps in the Metropolis as well as to the physical time of a real experiment. We refer to [36] for a detailed account of the Waiting Time Method. In all our runs, we conventionally

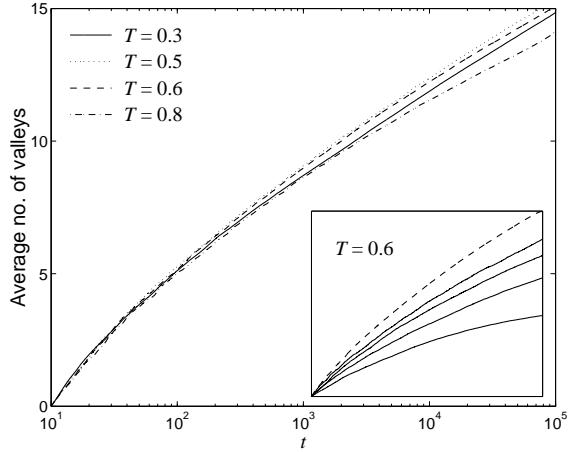


Figure 1: The average number of valleys  $n_V$  visited as a function of time in a  $N = 16^3$  gaussian spin glass. For  $t > 100$  a curvature is barely discernible. The insert shows  $n_V$  for system sizes  $L = 6, 8, 10$  and  $12$  (full lines), as well as  $L = 16$  (dashed line as in the main panel).

skip the data within the first 10 time units in order to let the system settle down from the random  $T = \infty$  initial configuration.

In ref. [13] the average number of barrier records  $\overline{n_B}(t)$  was shown to grow logarithmically in time, and the ratio of the variance  $\sigma_{n_B}^2(t)$  to  $\overline{n_B}(t)$  was found to be close to one. This implies that the statistics of barrier records is essentially a log-Poisson process, as expected in a record induced dynamics [14].

Figure 1 shows the average number of valleys  $\overline{n_V}(t)$  observed in the interval  $[10, t]$  for a number of different temperatures. In each case the average is performed over 30000 independent trajectories. Neglecting the earliest part of the simulations where the memory of the initial random spin configuration is still present,  $\overline{n_V}(t)$  has a logarithmic shape. On average, the ratio of the number of barrier records to minima records is therefore close to a constant. This non-trivial geometrical feature of the spin glass landscape has not previously been noted, and it provides a link to an analytical description of the non-equilibrium dynamics as a log-Poisson process [14].

The barely perceptible curvature seen in Fig. 1 for large  $t$  decreases systematically as the system size increases, as shown in the insert. The sub-

logarithmic form of  $\overline{n_V}(t)$  means that the likelihood that a bsf minimum follows a barrier record decreases very slowly, but systematically as the system ages. Taking into consideration that the curvature seems to vanish in the limit of a very large system, we surmise that its presence reflects the increasing difficulty in finding new bsf energies as the ground state is approached. In summary, the series of quakes moving the system from one valley to the next can be meaningfully idealized into a log-Poisson process discussed in the previous section, if one disregards the curvature of the data. How record events are distributed in time is insensitive to the properties of the stochastic process from which the records are drawn [14]. In our case Figs. 1 and 5 have a weak temperature dependence, as opposed to the strong  $T$  dependence of the underlying fluctuations.

The rest of this section deals with two scaling plots previously presented in ref. [13] (Figs. 2 and 4), as well as new results concerning the scaling of Hamming distances (Fig. 3) between the local minima of contiguous valleys. Finally, the statistics of the residence time and the fraction thereof spent before hitting the lowest energy state in the valley is analyzed.

#### 4.1 Barriers, Hamming distances and energies

The data shown in this section are averages over many thousands of realizations and cover a wide range of low temperatures and system sizes. The raw data for each  $T$  and  $N$  have very little scatter, and the main sources of error are systematic. For example, our finite runtimes, combined with the very broad distribution of residence times in the valleys, bias the average energy of valleys discovered late in the process, since only the 'faster' trajectories are able to explore these. The data are parametrized by the valley index  $i$ .

In our plots the scaling of the ordinate is given in the labels. The valley index  $i$  is shifted from one data set to another by up to one unit. This corresponds to a multiplicative shift of the age, and compensates for the arbitrariness of skipping data within the first 10 time units after the quench, irrespective of temperature and system size.

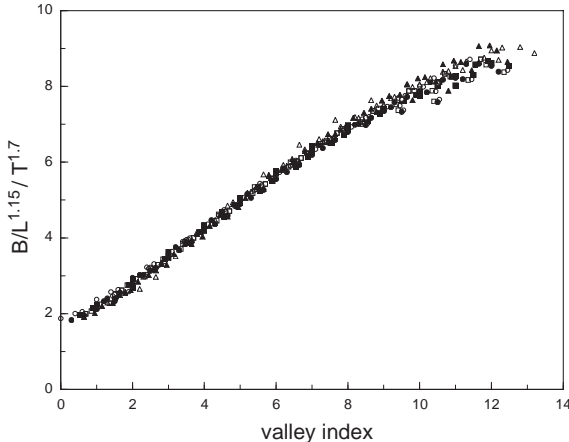


Figure 2: Average energy barrier records  $B$  separating contiguous valleys in  $N = L^3$  spin glass landscapes are scaled with  $L$  and  $T$  as indicated in the ordinate label and plotted versus the valley index. All combinations of  $L = 8, 10, 12, 14, 16$  and  $T = 0.3, 0.4, 0.5, 0.6$  and  $0.7$  are included, plus  $L = 18$  and  $T = 0.4$ .

Figure 2 is a scaling plot of the energy barrier  $B_i$  which on average must be surmounted in order to leave the  $i$ 'th valley.  $B_i$  is seen to scale in a simple way with the temperature and the size of the system:  $B_i = B_i(L^\alpha T^\beta)$ , where  $\alpha = 1.15$  and  $\beta = 1.70$ . Variations in the last digit of the exponents cause a visible worsening of the data collapse. The close to linear shape of the scaling plot shows that the barrier heights between valleys gradually increase.

Since  $\alpha > 1$ , the quakes do not remain localized to a finite set of spins in the limit  $L \rightarrow \infty$ . Some information on the size and shape of the quakes can be inferred from the scaling law for the energy barrier, if we assume that quakes correspond to the motion through the system of a generalized domain wall. Letting  $m$  be the number of spins typically involved in a quake, we write  $B \propto m^x$  for some exponent  $x > 0$ . Were the barrier energy simply the outcome of a fluctuation, i.e. the sum of  $m$  contributions of random sign, the behavior would be diffusion-like, with  $x = 1/2$ . However, since the barrier crossing process favors low-energy states, we expect a lower barrier energy, i.e.  $x < 1/2$ . Finally, since  $m \propto L^{1.15/x} \leq L^3$ , we conclude that  $x \in [0.38, 0.5]$ . In summary, quakes

have a fractal shape with exponent  $1.15/x$ , and are more space filling than a conventional domain wall.

An explanation of the  $T$  dependence of  $\beta$ , which deviates strongly from the Arrhenius form, involves entropic effects and the connection between the quasi-equilibrium dynamics in configuration space and in real space. The argument given below is only qualitative and predicts  $\beta = 2$  which is close to the found value of  $\beta = 1.7$ . The discrepancy might arise because we neglect that domain sizes are distributed quantities.

In real space, the relevant objects are connected domains [25, 37] of thermally equilibrated spins which slowly grow in a sea of frozen spins reaching, on average, a linear length scale  $\ell(t)$  on a time scale  $t$ . In the progressively longer quiescent periods between the quakes, these domains do not interact, and their quasi-equilibrium properties are therefore determined by the local density of states  $\mathcal{D}(E)$  pertaining to the configurations accessible to the spins constituting each domain.  $\mathcal{D}(E)$  has been investigated by means of the lid-algorithm [22] for a number of different glassy systems [23, 38, 39, 40, 41], and has consistently been found to have a close to exponential shape:  $\mathcal{D}(E) \approx \exp(E/T_0(\ell))$ . The energy scale  $T_0(\ell)$  is an upper bound for the temperature at which metastability can hold and decreases monotonically with the linear size  $\ell$  of the system considered [23]. While the results quoted pertain to systems of fixed size and shape, preliminary investigations confirm that the same behavior qualitatively persists if one considers spin domains of size  $\ell(t)$  which grow within a large system. In this case  $T_0(\ell)$  becomes a slowly decreasing function of time through the time dependence of  $\ell(t)$ , and asymptotically approaches  $T$  from above. We anticipate that the marginal stability of the valley visited implies that a domain is typically close to its maximal size, i.e.  $T_0(\ell(t)) \approx T$ .

Returning to  $B_i$ , we recall that energy barriers delimiting valleys are extremal values in a series of  $\mathcal{O}(t)$  independent outcomes in a system of age  $t$ , and that each attempt sees energy  $E$  with probability

$$P_{eq}(E) \approx \exp\left(-E \frac{T_0 - T}{T_0 T}\right). \quad (6)$$

It follows [42] that the typical energy barrier scales

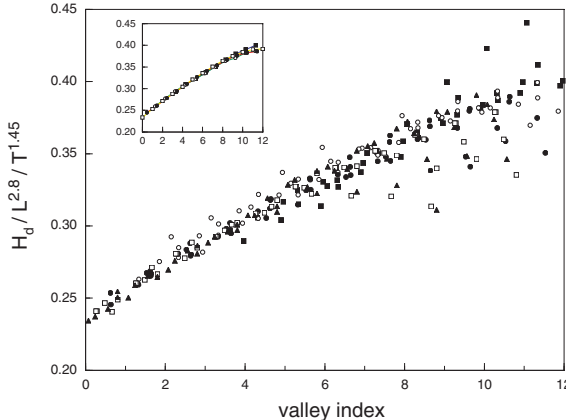


Figure 3: The average Hamming distance  $H_d$  between the lowest energy configuration of two contiguous valleys is plotted as a function of the valley index. All combinations of  $L = 8, 10, 12, 14, 16$  and  $T = 0.3, 0.4, 0.5, 0.6$  and  $0.7$  are included. In the insert we show data for  $L = 16$  and temperatures  $T = 0.3, 0.4, 0.5$  and  $0.6$ .

as

$$B_i \propto \frac{T_0 T}{T_0 - T} \log t. \quad (7)$$

Since the valley index grows linearly with  $\log t$ , the linear dependence on the valley index seen in Fig. 2 is recovered. Finally, since  $T_0 \approx T + \epsilon$  for some small  $\epsilon$ , one obtains  $\beta \approx 2$  as anticipated.

The fact that contiguous valleys contain rather different low energy configurations is shown in Fig. 3, which depicts the scaling of the Hamming distance  $H_d$  (number of spins which differ in their orientation) separating bsf configurations at the bottom of the two valleys. The data in the main panel are averages over 3000 independent runs, and the main sources of scatter are the poor scaling of the  $T = 0.3$  data (black squares) and the fact that smaller systems, mainly  $L = 8$ , systematically deviate from the linear trend observed for larger valley indices. The insert shows the same sort of temperature scaling but for one system size only,  $L = 16$ . These data are averaged over 30000 realizations and are completely smooth on the scale of the size of the symbols used.

The slight curvature of the data in Fig. 3 is a systematic consequence of the fact that the statistics for large valley indices is biased, resulting in  $H_d$  being

underestimated for larger  $i$ . If we could run the algorithm considerably longer, we might very well find the data on an almost straight line, just as we do for low  $i$ . This is true for Figs. 2 and 4 as well.

Interestingly, the data for  $T = 0.8$  (not shown) do not scale at all; the slope of the line is about twice as large as for the other temperatures. This tells us that the configurations selected differ considerably from those found at lower  $T$  values. Tentatively, a similar conclusion can be drawn from the scaling of the residence time statistics in Fig. 6. Obviously,  $T = 0.8$  is close to the critical temperature [43], where the quakes become so all-pervasive that the concept of a valley is of little value.

The strong temperature dependence of  $H_d$  in Fig. 3 is remarkable considering that the energies of the states involved are virtually independent of temperature, as implied by Fig. 4 and as one would expect for actual minima. It follows that the bsf states observed are nearly degenerate, which is also expected in spin glasses. The  $T$  dependence of  $H_d$  is likely due to the fact that higher barriers are overcome at higher  $T$ , and that the number  $m$  of spins involved in a quake is therefore larger. In the simplest scenario where the ‘downhill’ part of the quake does not substantially change  $m$ , one can assume  $m \propto H_d \propto L^{2.80}$ . The energy of the barrier state, which scales as  $B \propto L^{1.15}$ , must be carried by these  $m$  spins. Assuming that  $B \propto m^x \propto L^{2.80x}$  for some exponent  $x$ , we find  $x \approx 1.15/2.80 = 0.4$ . If the barrier energy were a sum of contributions of random sign one would expect  $x \approx 0.5$ , but a lower value is consistent with an expected bias toward lower energies.

The energy difference  $\Delta_i$  between the state of lowest energy in the first and the  $i$ ’th valley is plotted in Fig. 4. The linear trend observed means that the bsf energy decreases logarithmically with the age, a feature already implicit in the early investigations by Grest et al. [44]. The scatter of the data cannot be removed by an additional global scaling parameter, since data sets corresponding to different temperatures have slightly different shapes. The quality of the scaling deteriorates when data for  $T < 0.3$  are included.

The linear trend in Fig. 4 implies that the energy difference between neighboring valleys remains ap-

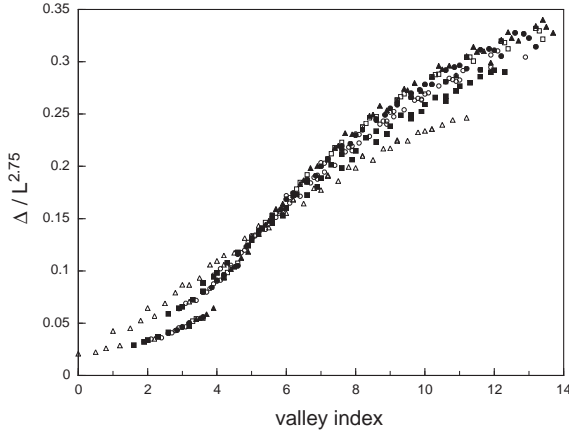


Figure 4: The average difference  $\Delta$  between the lowest energies found in the first and the  $i$ 'th valley is plotted versus  $i$ . The system and the combinations of  $L$  and  $T$  shown are as in the main panel of Fig. 2, except for an additional  $T = 0.2$  data set ( $\Delta$ ), which falls outside the main trend. The remaining spread in the data collapse cannot be removed by introducing an additional scaling parameter.

proximately constant along a trajectory. This means that the energy ‘gain’ induced by a quake per participating spin is of order  $L^{2.75}/L^{2.80} \approx \mathcal{O}(1)$ . In other words, the temperature determines the height of the barrier which must be overcome to enter a new valley, but it has no influence on the amount of bsf energy gained. Lowering the temperature only slows down the process of finding *similar* valleys.

We end the discussion of the scaling of the lowest energies in valleys by mentioning that the starting point  $E_1$  when measuring  $\Delta_i$  is only slightly  $T$ -dependent. If this was not the case, we could not claim the similarity of valleys as stated above. Finally, we conclude that our method of identifying valleys is physically sound, and that it produces simple scaling laws which give valuable information about the energy landscape.

## 4.2 Residence time distribution and superaging

The distribution of the time spent in ‘traps’ or valleys of the energy landscape has never been mea-

sured in simulations of model systems. Its assumed form enters heuristic scenarios of spin glass relaxation [45, 46], as well as to the log-Poisson description of non-equilibrium relaxation being developed in this paper.

Reintroducing the notation  $t_w$  for the age of the system, we consider the probability  $R(t \mid t_w)$  that the residence time  $t_r$  in a valley entered at age  $t_w$  be less than  $t$ . Some theoretical remarks on its expected form for a log-Poisson process are followed by a discussion of the simulation results.

Assuming a pure log-Poisson process, and for arbitrary  $t_w > 1$ , the ‘log waiting time’  $\ln(t_r + t_w) - \ln(t_w)$  is exponentially distributed with average  $1/\alpha$ , where  $\alpha = d\ln V/d\ln t$  is the logarithmic slope of Fig. 1. For any  $x > 0$ , the probability of  $t_r > t_w(e^x - 1)$  is therefore  $e^{-\alpha x}$ . Taking  $t = e^x - 1$ , the probability of  $t_r > tt_w$  is then given by  $(t + 1)^{-\alpha}$ , which is (trivially) the distribution of the age scaled residence time  $t_r/t_w$ . Since  $\alpha > 1$ , the distribution has the finite average  $\langle t_r \rangle = t_w/(\alpha - 1)$ .

The  $t_r/t_w$  scaling form is often called pure aging, as opposed to super- or sub-aging where the scaled variable is  $t/t_w^\mu$ , with  $\mu > 1$  or  $\mu < 1$ , respectively. Beside Fig. 5, superaging has been observed in some numerical investigations of spin glasses [47], while most experimental data show sub-aging [48, 49]. Very recent experimental work [35] shows that subaging is a consequence of the finiteness of the cooling rate. In the limit of a large cooling rate  $\mu$  approaches one and pure aging is obtained.

The empirical data of Fig. 5 are for  $N = 16^3$  spins and  $T = 0.4$ , and are averaged over 30000 runs with different realizations of the couplings  $J_{ij}$ . To study the age dependence, valleys entered in the time window  $[0.95t_w, 1.05t_w]$  are analyzed separately for several values of  $t_w$  taken from a broad range.

The figure confirms that the distribution of time spent in a valley moves to the right with  $t_w$ , and that, as shown in the insert, a  $t/t_w$  scaling is a fair approximation. The main panel shows that an excellent data collapse is obtained for  $R(t \mid t_w) = F(t/t_w^\mu)$  with  $\mu = 1.07(1)$ . Physically, this means that, compared to the idealized log-Poisson case, the residence time in a valley grows slightly faster than the age. This deviation from log-time homogeneity is likely

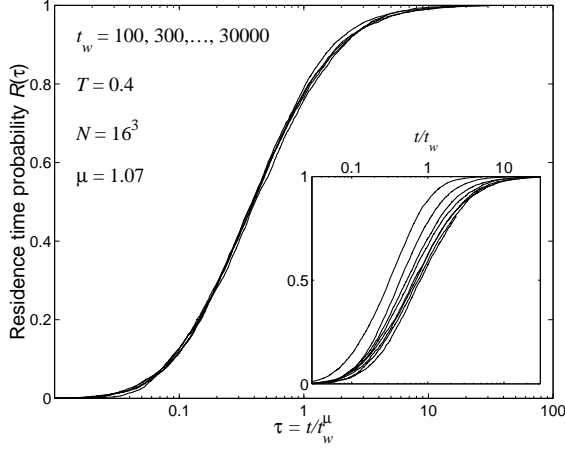


Figure 5: The main panel shows the probability that the residence time  $t_r$  is less than  $t$  for valleys entered in the time interval  $[0.95t_w, 1.05t_w]$  for a broad range of  $t_w$ . The abscissa is the scaled variable  $t/t_w^\mu$ . The insert shows that the pure aging  $t/t_w$  scaling predicted by log-Poisson statistics is a fair but far less satisfactory approximation.

due to the already mentioned fact that it becomes relatively harder to find a new valley as the ground state is approached.

With a  $T$  dependent exponent, the scaling  $t/t_w^{\mu(T)}$  works equally well for all temperatures up to  $T = 0.8$ , while the quality of the data collapse worsens at higher  $T$  values. The scaling plots obtained at different  $T$  are drawn together in Fig. 6. Since the logarithmic slope of these plots has a  $T$  dependence (the steepest curves belong to the highest temperatures), a perfect collapse is not achievable with the simple scaling form chosen. Still, the scaling accounts for most of the temperature dependence of the data, and to a good approximation

$$R(t | t_w, T) = F(t/t_w^{\mu(T)}). \quad (8)$$

The growth of the residence time with  $t_w^\mu$  shows that the valleys explored become more stable as the system grows older, which concurs with the growth law for the barriers given in Fig. 2.

The insert of Fig. 6 shows that  $\mu(T)$  increases linearly with  $T$ , i.e. the superaging effect becomes more pronounced as  $T$  increases. Noting that simulations slightly below the critical temperature, i.e. at the

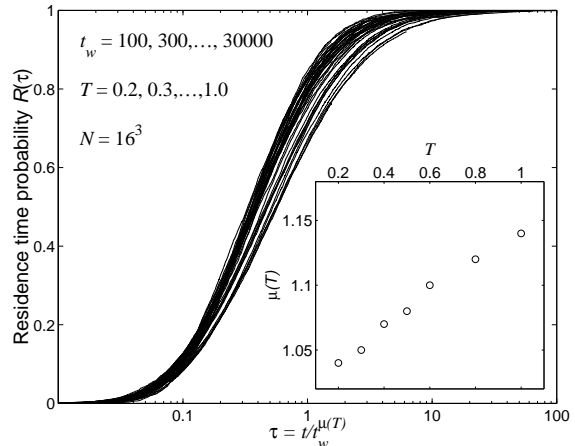


Figure 6: As in Fig. 5 but for a range of temperatures. The insert shows the temperature dependence of the exponent  $\mu$  used to scale the data for each temperature. Apart from a small but systematic change of steepness of the curves belonging to different temperatures, no temperature dependence other than in  $\mu(T)$  is observed.

high end of the low temperature phase, are able to explore lower energy regions in the same span of time, this strengthens our hypothesis that deviations from  $t/t_w$  scaling are a reverberation of the finiteness of the ground state energy. As such, these deviations can be expected to become less important the larger the system is. As a test, we ran 10000 simulations at  $T = 0.5$  on systems of size  $N = 30^3$ , finding  $\mu = 1.06(1)$  which is marginally, but significantly, lower than the corresponding value for a  $N = 16^3$  system shown in the insert of Fig. 6. Our interpretation also concurs with the experimental observation that pure aging emerges when cooling rate effects are properly accounted for [35].

### 4.3 Hitting time for the minima

Having argued that our method of partitioning the sampled states into valleys leads to consistent results and provides useful insight into the coarse structure of complex energy landscapes, it is natural to take a first look at the rich *internal structure* of the valleys. The existence of such a structure is implied by the wide distribution of residence times, which requires

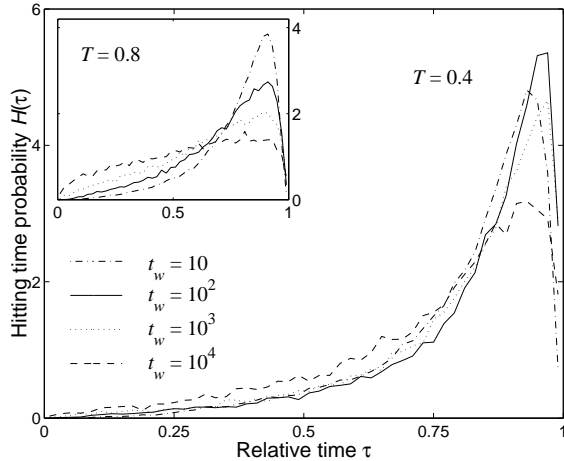


Figure 7: The location of the energy minimum within a valley entered at time  $t_w$ .  $N = 16^3$ . The abscissa is the time relative to the entry and exit times. The figure illustrates the highly right-skewed distribution found for all low  $T$ , independent of  $t_w$ . The insert shows that for higher  $T$  the distribution flattens out as the age of the system grows.

a matching distribution of internal energy barriers. Direct evidence is presented in this section, where we consider the 'hitting time'  $t_{hit}$  elapsing from the time of entry to the time where the lowest bsf state is encountered.

Consider  $\tau = t_{hit}/t_r$ , the fraction of the residence time spent 'searching' for the global minimum. We expect  $\tau$  to be close to zero in a structureless valley, where the global minimum is reached soon after entry, and close to one in the opposite limit of a rugged valley with many internal minima. In measuring the distribution of  $\tau$ , we keep track of the age at the time of entry, by selecting entry times to be in the interval  $[0.95t_w, 1.05t_w]$  for a range of different ages  $t_w$ . From the outset, the empirical distribution  $H(\tau | t_w)$  could depend on  $t_w$ , but, as shown by Fig. 7, there is practically no dependence, except for  $T$  close to the critical temperature.

The right-skewed form of  $H$  for lower  $T$  values (the picture is the same for any  $T \leq 0.6$ ) implies that by far the greatest part of  $t_r$  is spent before hitting the lowest minimum: the system explores several sub-valleys, each identified by its own local bsf

state, while it slides towards states of lower energy. Equilibrium-like fluctuations can only occur after the bsf energy which remains at the bottom of the valley is hit. This time interval is small compared to the total residence time, but nevertheless grows steadily with the valley index.

Since the measured shape of  $H$  is almost  $t_w$  invariant, the distributions of both  $t_r$  and  $t_{hit}$  must both scale as  $t_w^\mu$ . We conclude that the process of hitting the lowest minimum in a valley at low  $T$  is limited by internal barrier crossing events, and that these barriers themselves grow as the age increases and the valleys become larger. The landscape geometry is thus invariant under a time dilation, and hence self-similar, in agreement with the general properties of a log-Poisson process.

The temperature independence of the distribution leads to the same conclusion: Lowering the temperature means exploring smaller valleys, which nevertheless retain the same internal structure within a range of low temperatures. As the temperature gets closer to  $T_c$ , a slight waiting time dependence appears:  $H(\tau)$  remains peaked around  $\tau \simeq 0.9$ , but smaller values of  $\tau$  become gradually more probable. The corresponding flattening of the distribution of  $H(\tau)$  for  $T = 0.8$  is shown in the insert of Fig. 7.

## 5 Coarse grained landscape description

Having shown that log-Poisson statistics is a (slightly) idealized description which leads to pure aging and other dynamical features found in experiments, we turn to the physical mechanism behind the selection of the attractors and, more broadly, consider the implications of our results for pertinent mesoscopic models of complex landscapes. We do not attempt to deal with domain growth and other real space issues in any detail. These aspects, though very important for a complete understanding of complex relaxation, are too strongly connected to quasi-equilibrium issues which lie beyond the scope of this paper.

The applicability of log-Poisson statistics to *barrier*

records only implies that the trajectory fully decorrelates between successive events, as can be expected for an activated process in a landscape with many local minima. The new and important information about the landscape geometry lies in the fact that *barrier records are required in order to find new bsf minima*. This explains why the log-Poisson statistics is equally relevant for barriers as for minima. Secondly, and more importantly, it implies that the least stable, or *marginally* stable among the available attractors are those selected. Indeed, if at some stage, very deep minima were to follow a shallow barrier, subsequent barrier records would not produce new bsf states, and the log-Poisson description would fail.

The close match between the depth of a valley and the magnitude of the barrier record giving access to it implies a quasi-continuum of available attractors and was first noticed in connection with the noisy dynamics of a driven dissipative system [14], where the phenomenon was dubbed noise adaptation. That complex memory behavior is linked to marginal stability of metastable attractors has long been known for noiseless models of Charge Density Waves [15, 50]. The extremely simple automaton model of Tang et al. [50] describes a sheet of elastically coupled ‘balls’ driven along a sinusoidal potential by a pulsed external force. A recent study of a noisy version of this model [10] shows that its non-equilibrium dynamics is described by log-Poisson statistics and that the age of the system can be reset by a change of the elastic coupling constant.

The physical origin of the bias towards shallow attractors in thermal glassy dynamics is likely to be entropic, i.e. simply the fact that shallow attractors vastly outnumber deeper ones, in line with the general observation that quenches usually produce poor minima. To support such bias for a range of low temperatures, the density of energy minima must dwarf the Boltzmann factor and hence increase at least exponentially with the energy. This concurs with the outcome of numerical exhaustive investigations of the local configuration space structure of different glassy systems [22, 23, 38, 40, 41, 51, 52] which were performed with the lid method [22, 39]. In all cases the local density of states and the local density of minima are nearly exponential functions of the energy.

An exponential density of states in connection with activated dynamics implies a dynamical glass transition. This exact feature was built into the tree model of complex relaxation proposed and analyzed by Grossmann et al. [53] and later studied in more detail in [54, 55]. It is also incorporated in the even simpler trap model of Bouchaud [45] which, nonetheless, is very different from tree models in one important respect: trees have the lowest connectivity possible for a connected set, while each trap of the trap model is connected to all others.

Log-Poisson statistics only applies as long as new and gradually more stable valleys remain available to the dynamics. The simplest way of modeling inequivalent valleys is through a hierarchy of energy barriers separating degenerate states, which are organized in either a linear array [56] or in a tree graph. Beside the models already mentioned, the latter approach is followed in [55, 56, 57, 58, 59, 60]. Many important features of complex relaxation can be reproduced in this model, but not the fact that in many systems, including spin glasses, the energy decreases logarithmically with the age. This can be achieved by introducing non-degenerate local minima, as done in the so-called LS tree [7, 61]. The minima have energies which on average decrease linearly with the size of the barrier overcome, i.e. in the same overall fashion as Fig. 4.

In Bouchaud’s model, trap energies are exponentially distributed and hence non-degenerate. That deeper minima are gradually explored is a statistical consequence of the (assumed) infinite average of the residence time in a trap. If traps and valleys can be identified, the results of Section 4.2 are at variance with this interpretation. The average residence time, which equals  $t_w$  for  $\alpha = 2$ , is, in practice, slightly lower than  $t_w$ . This is again reminiscent of the situation encountered in tree models [7, 55, 57, 58, 59, 60, 61]. The distribution of barriers in tree models has a lower cut-off, unlike the fractal description of configuration space of Dot-senko [62, 63], which better captures the growing importance of gradually smaller barriers as the temperature decreases.

A last important issue is the connection between the energy barrier separating two configurations and

the distance between them. For spin glasses the relevant metric is the Hamming distance, which, according to Figs. 3 and 4, on average bears a linear relationship to the energy barrier. A similar result was found in numerical work on the SK model [64] by [18, 65], and by the lid-method (i.e. exact exhaustive enumeration) in [38] for short range spin glasses. Since the latter investigations deal with the small scale structures inside a ‘pocket’, while the present ones are concerned with the large scale structures explored by the non-equilibrium dynamics, the agreement in their outcome is further evidence for a self-similar landscape structure. Interestingly, the *largest* distance which can be achieved for a fixed energy barrier grows exponentially with the barrier [23]. A linear relationship between energy and Hamming distance is assumed in tree models of aging dynamics, see e.g. [59], and also in the barrier model [56]. This is, however, not a crucial assumption for aging, and other types of functional relationships can also be utilized [7] successfully.

## 6 Summary and outlook

In this paper we have presented a general ‘non-invasive’ statistical method for complex energy landscape exploration, especially designed to provide information on the metastable states actually explored by an unperturbed aging process following a quench. The method has been thoroughly tested on short range spin glasses, and the results obtained both match and extend the established knowledge about spin glasses. The view which emerges is that non-equilibrium aging dynamics is steered by energy barrier *records*, which are the only events capable of opening the route to new valleys. Since this description has previously been shown to apply to driven dissipative models and to evolution modeling, a possible unified theory for non-equilibrium glassy dynamics seems within reach.

A more complete picture can be obtained by looking more closely into the fluctuation dynamics which may differ across different systems. For spin glasses we have argued that real space domains of (pseudo) thermalized spins relax independently as long as the

system as a whole remains in the same valley. The present method opens the possibility of identifying the quasi-equilibrium clusters as defined by the dynamics itself: These clusters are separated by a backbone of spins whose orientation remains fixed within each valley and changes slowly from one valley to the next, as seen in Fig. 3. After the lowest energy state in the valley has been hit and before the next valley is entered, there is no drift towards the global minimum. Hence, the spins fall into two categories only: those which are frozen, and those which fluctuate in a quasi-equilibrium fashion. The quasi-equilibrium clusters can thus be extracted and their statistical properties, such as e.g. the density of states, can be studied for each cluster separately.

**Acknowledgments:** This project has been supported by Statens Naturvidenskabelige Forskningsråd through a block grant and by the Danish Center for Super Computing with computer time on the Horseshoe Linux Cluster. We are grateful to J. Christian Schön for many discussions, and, in particular, for pointing out a flawed mathematical argument in an early version of this work.

## References

- [1] W. Reim, R. H. Koch, A. P. Malozemoff, M. B. Ketchen, and H. Maletta. Magnetic Equilibrium Noise in Spin-Glasses:  $\text{Eu}_{0.4}\text{Sr}_{0.6}\text{S}$ . *Phys. Rev. Lett.*, 57:905–908, 1986.
- [2] Ph. Refrigier and M. Ocio. Measurement of spontaneous magnetic fluctuations. *Revue Phys. Appl.*, 22:367–374, 1987.
- [3] J-O. Andersson, J. Mattsson, and P. Svedlindh. Monte Carlo studies of Ising spin-glass systems: Aging behavior and crossover between equilibrium and nonequilibrium dynamics. *Phys. Rev. B*, 46:8297–8304, 1992.
- [4] P. Granberg, L. Sandlund, P. Nordblad, P. Svedlindh, and L. Lundgren. Observation of a time-dependent spatial correlation length in a

metallic spin glass. *Phys. Rev. B*, 38:7097–7100, 1988.

[5] P. Granberg, L. Lundgren, and P. Nordblad. Non-equilibrium relaxation in a Cu(Mn) spin glass. *J. Magn. and Magnetic Materials*, 90:228–232, 1990.

[6] C. Schultze, K. H. Hoffmann, and P. Sibani. Aging phenomena in complex systems: A hierarchical model for temperature step experiments. *Europhys. Lett.*, 15:361–366, 1991.

[7] K.H. Hoffmann, S. Schubert, and P. Sibani. Age reinitialization in spin-glass dynamics and in hierarchical relaxation models. *Europhys. Lett.*, 38:613–618, 1997.

[8] A. V. Kityk, M. C. Rheinstädter, K. Knorr, and H. Rieger. Aging and memory effects in  $\beta$ -hydrochinone-clathrate. *Phys. Rev. B*, 65:14415, 2002.

[9] Mario Nicodemi and Henrik Jeldtoft Jensen. Aging and memory phenomena in magnetic and transport properties of vortex matter: a brief review. *J. Phys. A*, 34:8425, 2001.

[10] P. Sibani and C. M. Andersen. Aging and self-organized criticality in driven dissipative systems. *Phys. Rev. E*, 64:021103, 2001.

[11] L. Bureau, T. Baumberger, and C. Caroli. Rheological aging and rejuvenation in solid friction contacts. *cond-mat/0202245*, 2002.

[12] A. Hannemann, J. C. Schön, M. Jansen, and P. Sibani. Non-equilibrium dynamics in amorphous  $\text{Si}_3\text{B}_3\text{N}_7$ . *cond-mat/0212245*, 2002.

[13] Paolo Sibani and Jesper Dall. Extracting the Landscape and Morphology of Aging Glassy Systems. *cond-mat/0206535*, 2002.

[14] P. Sibani and Peter B. Littlewood. Slow Dynamics from Noise Adaptation. *Phys. Rev. Lett.*, 71:1482–1485, 1993.

[15] S.N. Coppersmith and P.B. Littlewood. Pulse-duration memory effect and deformable charge-density waves. *Phys. Rev. B*, 36:311–317, 1987.

[16] K. Jonason, E. Vincent, J. Hamman, J. P. Bouchaud, and P. Nordblad. Memory and Chaos Effects in Spin Glasses. *Phys. Rev. Lett.*, 81:3243–3246, 1998.

[17] Frank H. Stillinger and Thomas A. Weber. Dynamics of structural transitions in liquids. *Phys. Rev. A*, 28:2408–2416, 1983.

[18] K. Nemoto. Metastable states of the SK spin glass model. *J. Phys. A*, 21:L287–L294, 1988.

[19] Oren M. Becker and Martin Karplus. The topology of multidimensional energy surfaces: Theory and application to peptide structure and kinetics. *J. Chem. Phys.*, 106:1495–1517, 1997.

[20] A. Crisanti and F. Ritort. Inherent structures, configurational entropy and slow glassy dynamics. *J. of Phys. Cond. Matt.*, 14:1381–1395, 2002.

[21] S. Mossa, G. Ruocco, F. Sciortino, and P. Tartaglia. Quenches and crunches: does the system explore in ageing the same part of the configuration space explored in equilibrium? *Phil. Mag. B*, 82:695–705, 2002.

[22] P. Sibani, C. Schön, P. Salamon, and J.-O. Andersson. Emergent hierarchical structures in complex system dynamics. *Europhys. Lett.*, 22:479–485, 1993.

[23] P. Sibani. Local state space geometry and thermal relaxation in complex landscapes: the spin-glass case. *Physica A*, 258:249–262, 1998.

[24] J. C. Schön, H. Putz, and M. Jansen. Studying the energy hypersurface of continuous systems—the threshold algorithm. *J. Phys.: Condens. Matter*, 8:143–156, 1996.

[25] J.-O. Andersson and P. Sibani. Domain growth and thermal relaxation in spin glasses. *Physica A*, 229:259–272, 1996.

[26] Matteo Palassini and A. P. Young. Triviality of the Ground State Structure in Ising Spin Glasses. *Phys. Rev. Lett.*, 83:5126–5129, 1999.

[27] J. Houdayer and O. C. Martin. A geometrical picture for finite-dimensional spin glasses. *Europhys. Lett.*, 49(6):794–800, 2000.

[28] J. Lamarcq, J. P. Bouchaud, O. C Martin, and M. Mezard. Non-compact local excitations in spin glasses. *Europhys. Lett.*, 58:321–327, 2002.

[29] M. A. C. Wevers, J. C. Schön, and M. Jansen. Global aspects of the energy landscape of metastable crystal structures in ionic compounds. *J. Phys.:CONDENS. Matter*, 11:6487–6499, 1999.

[30] P. Sibani, M. Schmidt, and Preben Alstrøm. Fitness optimization and decay of the extinction rate through biological evolution. *Phys. Rev. Lett.*, 75:2055–2058, 1995.

[31] P. Sibani, M. Brandt, and P. Alstrøm. Evolution and extinction dynamics in rugged fitness landscapes. *Int. J. Modern Phys. B*, 12:361–391, 1998.

[32] P. Sibani and A. Pedersen. Evolution dynamics in terraced NK landscapes. *Europhys. Lett.*, 48:346–352, 1999.

[33] S. A. Kauffman and S. Levine. Towards a general theory of adaptive walks in rugged landscapes. *J. Theor. Biol.*, 128:11–45, 1987.

[34] Matt Hall, Kim Christensen, Simone A. di Colabiano, and Henrik J. Jensen. Time dependent extinction rate and species abundance in the Tangled Nature model of biological evolution. *Phys. Rev. E*, 66:011904, 2002.

[35] G. F. Rodriguez, G. G. Kenning, and R. Orbach. Full Aging in Spin Glasses. *cond-mat/0212259*, 2002.

[36] Jesper Dall and Paolo Sibani. Faster Monte Carlo simulations at low temperatures. The waiting time method. *Comp. Phys. Comm.*, 141:260–267, 2001.

[37] J. Kisker, L. Santen, M. Schreckenberg, and H. Rieger. Off-equilibrium dynamics in finite-dimensional spin-glass model. *Phys. Rev. B*, 53:6418–6428, 1996.

[38] P. Sibani and P. Schriver. Phase-structure and low-temperature dynamics of short range Ising spin glasses. *Phys. Rev. B*, 49:6667–6671, 1994.

[39] P. Sibani, R. van der Pas, and J. C. Schön. The lid method for exhaustive exploration of metastable states of complex systems. *Computer Physics Communications*, 116:17–27, 1999.

[40] J. C. Schön and P. Sibani. Properties of the energy landscape of network models for covalent glasses. *J. Phys. A*, 31:8165–8178, 1998.

[41] J. C. Schön and P. Sibani. Energy and entropy of metastable states in glassy systems. *Europhys. Lett.*, 49:196–202, 2000.

[42] M. R. Leadbetter, Georg Lindgren, and Holger Rootzen. *Extremes and related properties of random sequences and processes*. Springer-Verlag, New York Heidelberg Berlin, 1983.

[43] Marco Picco, Federico Ricci-Tersenghi, and Felix Ritort. Chaotic, memory, and cooling rate effects in spin glasses: Evaluation of the Edwards-Anderson model. *Physical Review B*, 63:174412, 2001.

[44] G. S. Grest, C. M. Soukoulis, and K. Levin. Cooling Rate Dependence for the Spin Glass Ground State Energy: Implications for Optimization by Simulated Annealing. *Phys. Rev. Lett.*, 56:1148–1151, 1986.

[45] J.P. Bouchaud. Weak ergodicity breaking and aging in disordered systems. *J. Phys. I France*, 2:1705–1713, 1992.

[46] E. Vincent, J. P. Bouchaud, D. S. Dean, and J. Hammann. Aging in spin-glasses as a random walk: effect of a magnetic field on the landscape. *Phys. Rev. B*, 52:1050–1060, 1995.

[47] Ludovic Berthier and Jean-Philippe Bouchaud. Geometrical Aspects of Aging and Rejuvenation in the Ising Spin Glass: A Numerical Study. *cond-mat/0202069*, 2002.

[48] Eric Vincent, Jacques Hammann, Miguel Ocio, Jean-Philippe Bouchaud, and Leticia F. Cugliandolo. Slow Dynamics and Aging in Spin Glasses. In Miquel Rubí and Conrado Pérez-Vicente, editors, *Lecture notes in physics: Complex Behaviour of Glassy Systems*, volume 492, pages 184–219. Springer, 1997.

[49] J-P Bouchaud. Aging in glassy systems: new experiments, simple models, and open questions. In M. E. Cates and M. R. Evans, editors, *Soft and Fragile Matter*, pages 285–304, 1999.

[50] Chao Tang, Kurt Wiesenfeld, Per Bak, Susan Coppersmith, and Peter Littlewood. Phase Organization. *Phys. Rev. Lett.*, 58:1161–1164, 1987.

[51] T. Klotz, S. Schubert, and K. H. Hoffmann. Coarse Graining of a Spin-Glass State Space. *Journal of Physics-Condensed Matter*, 10:6127–6134, 1998.

[52] J.C. Schön. The energy landscape of two-dimensional polymer. *J. Phys. Chem. A*, 106:10886–10892, 2002.

[53] S. Grossmann, F. Wegner, and K. H. Hoffmann. Anomalous diffusion on a selfsimilar hierarchical structure. *J. Physique Letters*, 46:575–583, 1985.

[54] K.H. Hoffmann, S. Grossmann, and F. Wegner. Random walk on a fractal. *Z. Phys. B*, 60:401–414, 1985.

[55] P. Sibani. Anomalous diffusion and low-temperature spin-glass susceptibility. *Phys. Rev. B*, 35:8572–8578, 1987.

[56] Y. G. Joh, R. Orbach, and J. Hamman. Spin Glass Dynamics under a Change in Magnetic Field. *Phys. Rev. Lett.*, 77:4648–4651, 1995.

[57] M. Schreckenberg. Long range diffusion in ultrametric spaces. *Z. Phys. B*, 60:483–488, 1985.

[58] Paolo Sibani. Random walks on Cayley trees as models for relaxation in a hierarchical system. *Phys. Rev. B*, 34:3555–3558, 1986.

[59] Paolo Sibani and Karl Heinz Hoffmann. Hierarchical models for aging and relaxation in spin glasses. *Phys. Rev. Lett.*, 63:2853–2856, 1989.

[60] K.H. Hoffmann and P. Sibani. Relaxation and aging in spin glasses and other complex systems. *Z. Phys. B*, 80:429–438, 1990.

[61] P. Sibani and K.H. Hoffmann. Relaxation in complex systems : local minima and their exponents. *Europhys. Lett.*, 16:423–428, 1991.

[62] Vik S. Dotsenko. Fractal dynamics of spin glasses. *J. Phys. C*, 18:6023–6031, 1985.

[63] E. Vincent. Slow dynamics in spin glasses and other complex systems. In D. H. Ryan, editor, *Recent progress in random magnets*, pages 209–246. Mc Gill University, 1991.

[64] David Sherrington and Scott Kirkpatrick. Solvable model of a spin-glass. *Phys. Rev. Lett.*, 35:1792–1796, 1975.

[65] D. Vertechi and M.A. Virasoro. Energy barriers in SK spin-glass model. *J. Phys. France*, 50:2325–2332, 1989.